



**Sudan University of Science and Technology**

**College of Graduate Studies**

**Measurement of Common Bile Duct and Pancreatic Duct for  
obstructive jaundice using Magnetic Resonance**

**Cholangiopancreatography (MRCP)**

**قياس القناة الصفراوية والبنكرياسية المشتركة لليرقان الانسدادي**

**باستخدام الرنين المغناطيسي**

*A thesis submitted for partial fulfillment of the requirements*

*Of M.Sc. Degree in Diagnostic Radiologic Technology*

**By:**

**Rofida Mahmoud Abdomohamedsalih**

**Supervisor:**

**Dr. Mona Ahmed Mohamed**

**Associate professor**

**2018**

الاية

( فَتَعَالَى اللَّهُ الْمَلِكُ الْحَقُّ وَلَا تَعْجَلْ بِالْقُرْآنِ مِنْ قَبْلِ أَنْ

يُقْضَى إِلَيْكَ وَحْيُهُ وَقُلْ رَبِّ زِدْنِي عِلْمًا )

صدق الله العظيم

سورة طه (114)

# Dedications

I would like to dedicate my thesis to:

The tender man ...

My Father

The Kindest woman ...

My Mother

To my dearest friends

## **Acknowledgments**

I would like to express my greatest gratitude to **Dr .Mona AHmed Mohamed for** her supervising this work to layout.

My thanks are extended to my friend

(MujahidMohmed.Zidan&MarwaMohamedYousef, Awdyia Mohamed Ahmed, Tassbih Al-ride) for their helps.

My gratitude is also extended to my colleagues in RadiologyDepartment at Teaching medical city and Royal Scan Diagnostic Centerfor their continuous help and support.

Finally, my profound thanks and gratitude to everyone whoencouraged me to complete this thesis.

## Abstract

This descriptive cross-sectional study aimed to measure the diameter of the common bile duct and pancreatic duct in obstructive jaundice and correlate this measurement with age and gender.

The study done for 55 patients 16 male and 39 female their age between (21 -78) years, they selected randomly when they attended to radiology department for performed MRCP. The diameter of common bile duct and pancreatic duct were measured from the 2D images of (SSTSE BH). Then the data analyzed by SPSS to find the mean and standard deviations correlations.

The study found the mean of the diameter common bile duct for female & male of age group (21-78) years were (5.8±2.0 mm) of male and (6.9±4.7mm) of female , and the diameter of pancreatic duct were (2.3±0.4mm) for male and were (2.5±0.8mm) for female respectively.

In addition, the study found correlation between the diameter of common bile duct and pancreatic duct and age statistically on significant for both male and female were no significant of values R (0.68 and 0.11) respectively.

The study concluded that the diameter of common bile duct and pancreatic duct of obstructive jaundice was same to compared male and female there were no significant difference.

The study recommended further studies in measuring common bile duct and pancreatic duct with larger sample of population.

## ملخص البحث

هذه الدراسة الوصفية تهدف إلى قياس قطر القناة الصفراوية المشتركة والقناة البنكرياسية في اليرقان الانسدادي وترتبط هذا القياس مع العمر والجنس.

أجريت الدراسة على 55 مريضاً 16 ذكراً و 39 عاماً في عمرهم بين (21\_ 78) عاماً ، وقد اختاروا بشكل عشوائي عندما حضروا إلى قسم الأشعة لإجراء MRCP. تم قياس قطر القناة الصفراوية المشتركة والقناة البنكرياسية من الصور ثنائية الأبعاد لـ (SSTSE BH). ثم تحليل البيانات بواسطة SPSS للعثور على الارتباطات الانحرافات المتوسطة والمعايير.

وجدت الدراسة أن متوسط القناة الصفراوية العامة للذكور والإناث من الفئة العمرية (21-78) سنة (5.8 ± 2.0 مم) من الذكور و (6.9 ± 4.7 ملم) من الإناث ، وقطر القناة البنكرياسية كانت (2.3 ± 0.4 mm) للذكور وكانت (2.5 ± 0.8 mm) للإناث على التوالي.

بالإضافة إلى ذلك ، وجدت الدراسة العلاقة بين قطر القناة الصفراوية المشتركة والقناة البنكرياسية وعمرها إحصائياً على كل من الذكور والإناث من حيث القيمة النانوية للقيم R (0.68 و 0.11) على التوالي.

وخلصت الدراسة إلى أن قطر القناة الصفراوية المشتركة ومجرى القناة البنكرياسية من اليرقان الانسدادي هو نفسه مقارنة بالذكور والإناث إحصائياً غير مختلفه.

أوصت الدراسة بمزيد من الدراسات في قياس القناة الصفراوية والقناة البنكرياسية مع عينة أكبر من السكان.

## List of Table

(4.1)	demonstrate the distribution of the gender	45
(4.2)	Demonstrate measurement of (male and female) in both Common Bile Duct and Pancreatic Duct according to Gender.	46
(4.3)	Demonstrate measure of effect of age to (CBD) and (PD) and coefficients test.	46
(4.4)	Demonstrate measurement of common bile duct and pancreatic duct according to age.	47
(4.5)	Demonstrate of Independent samples test for equality of means of males and females in both (CBD) and (PD).	47

## List of Figures

<b>Figure</b>	<b>Title</b>	<b>Page</b>
(2.1)	Shows liver segments	5
(2.2)	Shows intrahepatic bile ducts	7
(2.3)	Shows biliary confluence	9
(2.4)	Shows anatomy of the extrahepatic biliary system	12
(2.5)	Shows blood supply to the extrahepatic bile ducts.	14
(2.6)	Shows scanning range prescription for the axial 2D SSFSE Fat show suppressed series.	28
(2.7)	Shows scanning range prescription for the Coronal 2D SSFSE Fat Suppressed sequence in: The diagnostic MRCP examination	29
(2.8A)	Shows First slice prescribed coronal, directly through the CBD.	30
(2.8B)	Shows indicates the second prescribed slice parallel to the cystic duct.	30
(2.8C)	Shows indicates how the third slice prescribed parallel to the main pancreatic duct through the head of pancreas.	31
(2.9)	Shows volume prescription for the Para-coronal 3D MRCP Respiratory Triggered sequence.	32
(4.1)	Shows demonstrate the distribution of the gender.	45
(4.2)	Shows the measurement of the mean in Common bile duct and pancreatic according the gender.	46
(4.3)	Shows the plots the regression of common bile duct and pancreatic duct according the age	46

## List of abbreviations



<b>MRI</b>	Magnetic Resonance Imaging
<b>ERCP</b>	endoscopic retrograde pancreato-chole angiography
<b>MPI</b>	maximum intensity projection
<b>SSFP</b>	steady state free precession
<b>FSE</b>	Fast spin echo
<b>SNR</b>	signal to noise ratio
<b>CNR</b>	contrast to noise ratio
<b>PV</b>	Portal vein
<b>HA</b>	Hepatic Artery
<b>HV</b>	Hepatic veins
<b>IHBD</b>	Intra hepatic bile ducts
<b>GB</b>	Gallbladder
<b>CBD</b>	Common Bile Duct
<b>FLASH</b>	Fast low angle shot
<b>MRCP</b>	Magnetic resonance cholepancreatography
<b>GD</b>	Gall bladder

## List of Contents

Topic	Page
الآية	I
Dedication	II
Acknowledgment	III
Abstract English	IV
Abstract Arabic	V
List of Tables	VI
List of Figures	VIII
List of Abbreviation	IX
Contents	XI
<b>Chapter One: Introduction</b>	
1.1 Introduction	1
1.2 Research problems	2
1.3 objectives of the study	2
1.4 Research Overview	2
<b>Chapter Two: Theoretical Background and previous study</b>	
2.1:Theoretical Background	3
2.1.1:Anatomy of the Biliary System	3
2.1.2:Liver anatomy	3
2.1.3:Intra hepatic bile ducts (IHBD)	6
2.1.4:Extrahepatic biliary duct	9
2.1.5: The pancreas	14
2.1.6: Physiologic Anatomy of Biliary Secretion	17
2.1.7: Pathology of the liver, biliary system, and pancreas	18

2.1.8: MRCP technique	25
2.2 previous studies	34
<b>Chapter Three :Materials and Methods</b>	
3.1 Materials	36
3.2 Methods	36
<b>Chapter Four :Results</b>	
4.1 Results	38
<b>Chapter Five :Discussion, Conclusion and Recommendations</b>	
5.1 Discussion	45
5.2 Conclusion	47
5.3 Recommendations	48
References	49
Appendix	51

# **Chapter One**

# Chapter One

## 1.1 Introduction:

Magnetic resonance cholangiopancreatography MRCP noninvasive radiographic technique that make an image of pancreaticobiliary tree similar to endoscopic retrograde pancreato-chole angiography (ERCP). (Earls 2002).

MRCP allow pancreatic and biliary anatomy to be defined noninvasively, without risk of pancreatitis and radiation exposure, and may detect micro-lithiasis, choledocholithiasis, unsuspected chronic pancreatitis, and, in some cases, pancreas divisum and annular pancreas. Therefore, MRCP is an appropriate noninvasive tool for suspected pancreatic biliary pathology (Zaliekas and Munson. 2008).

The basic Principle of MRCP is body fluid such as bile and pancreatic secretion had high signal (appear white) on heavy T2 weighted image (echo time longer than 150ms) and the tissue around were markedly suppressed; no signal from flowing blood. This source image obtained in any plane and form volumetric data set suitable for further analysis, especially reformatting algorithm such as maximum intensity projection (MPI) and shaded source display (Gulati et al. 2007) Several technique were used in MRCP, first 2D T2 weighted gradient echo sequence with steady state free precession (SSFP) during breath hold , this sequence was subsequently optimized using 3D acquisition volume. Alexander Fast spin echo (FSE) sequence demonstrated as a very suitable for performing heavy T2Weighted studies in abdomen. FSE sequence compared with gradient echo GRE sequence: FSE had higher signal to noise ratio (SNR), contrast to noise ratio (CNR) lower sensitivity to susceptibility artifacts, motion artifact and blood flow. (Lee. et al 2000)

Also, improve image quality such as gradient moment nulling, which reduce artifact from periodic motion, respiratory triggering. Fat Suppression technique

additionally improve contrast between bile duct and back ground in breath hold and non-breath hold technique with similar result(Alexander, et al).

## **1.2 Problem of study:**

There is no stander measurement of common bile duct and pancreatic duct for Sudanese using to diagnosis biliary system abnormality.

## **1.3 objectives of the study:**

### **1.3.1 General objective:**

Measurement of common bile duct and pancreatic duct in adults using Magnetic Resonance cholangiopancreatography (MRCP)

### **1.3.2 Specific objectives:**

1. To correlate between common bile duct and Pancreatic duct measurement with gender
2. To correlate between common bile duct and Pancreatic duct measurement age

## **1.4 The overview of the study:**

The general framework of this research is built in five chapter's asFollows:

Chapter one: dealing with introduction and objectives of research.

Chapter two: dealing with literature review.

Chapter three: dealing with materials and methods.

Chapter four: dealing with result.

Chapter five: dealing with discussion, conclusion andrecommendations.

## **Chapter Two**

### **Theoretical Background and Previous studies**

## **Chapter Two**

### **Theoretical Background and Previous studies**

#### **2.1: Theoretical Background:**

##### **2.1.1: Anatomy of the Biliary System:**

The liver, biliary tree and the gallbladder occupy the right upper quadrant of the abdomen. The liver resides between the digestive tract and the rest of the body and functions as a way station between the splanchnic and systemic circulation (Kumar et al .2004).

It is composed largely of epithelial cells (hepatocytes), which passed in blood derived from the hepatic portal veins and hepatic arteries. There are continuous chemical exchange between the cells and the blood. Hepatocytes are also associated with an extensive system of minute canals, which form the biliary system into which products are secreted (Standring.2008).

The biliary tract conduit between the liver and the duodenum and designed to store and transport bile, under control of neuronal and hormonal regulation. Bile formed in the hepatocytes and steadily secreted into canaliculi, which transport it to the larger extrahepatic ducts. The sphincter of Oddi regulates the flow of bile into the duodenum or to the cystic duct and the gallbladder (Pierre and Laillie. 2014).

##### **2.1.2: Liver anatomy:**

The mature liver lies in the right hypochondrium under the rib cage and extends from the right fifth intercostal space at the midclavicular line to just below the costal margin. It projects slightly below the costal margin at right intercostal line under the xyphoid process in the midline (Kumar et al.2004).

To understand anatomy and physiology of biliary tract and bile production, it necessary to outline briefly the anatomy of the liver. The liver divided



microscopically into right and left lobe by falciform ligament anteriorly. Inferiorly, this corresponds to the round ligament and umbilical fissure. The right lobe further divided by gallbladder fossa into right hemi liver to the right of the gallbladder and quadrate lobe to the left. The fourth lobe (caudate) which lies posterior and surrounds inferior vena cava. Hence, anatomically the liver divided into two main lobes and two accessory lobes. (Pierre and Laillie. 2014).

### **2.1.3: Liver segmentation**

With improved understanding of liver function, the concept of functional anatomy has developed. In December 1998, a Scientific Committee of the International Hepato-Pancreato-Biliary Association created a terminology called The Brisbane 2000 Terminology of Liver Anatomy and Resection. Estimate that, the liver divided into three functional livers: right, left and the caudate. (Pierre and Laillie. 2014). The separation between the right and left hemiliver is at Cantlie's line, which is an oblique plane extending from the center of the gallbladder bed to the left border of the inferior vena cava. In this plane runs the middle hepatic vein, The Right hemi liver divided further into two sections by the right portal scissura (anterior and posterior sections), within which runs the right hepatic vein. Each section then divided based on their blood supply and bile drainage into two segments (figure 2.1) (segment V & VIII anterior and segment VI & VII posterior). The left hemi liver divided into three segments (segment IV, III, & II). The caudate hemi liver (segment I) considered separately because of its separate blood supply and venous and bile drainage. (Pierre and Laillie. 2014).

### **2.1.4: Blood supply and venous drainage**

The vessels connected with the liver are the portal vein, hepatic artery and hepatic veins. The portal vein and hepatic artery ascend in the lesser omentum to the porta hepatic, where each bifurcate. About One-fourth of the blood and one-half the

oxygen come by way of the hepatic artery. The remainder was been carried by the portal vein. (Skandalaki.et al 2008).

The hepatic artery in adult, is intermediate in size between the left gastric and splenic arteries. In fetal and early postnatal life, it is the largest branch of coeliac axis. After its origin from the coeliac axis, it passes anteriorly and laterally below the epiploic foramen to the upper aspect of superior part of the duodenum. The artery may be subdivided into common hepatic artery - from the coeliac trunk to the origin of the gastroduodenal artery -and the hepatic artery 'proper - from that point to its bifurcation. It passes anterior to the portal vein and ascends between the layers of the lesser omentum. It lies anterior to epiploic foramen and passes in free border of Lesser omentum medial to common bile duct and anterior to portal vein. (Skandalaki.et al 2008).

At porta hepatic, the hepatic artery divides into right and left branches before these run into the parenchyma of the liver. The right hepatic artery usually crosses posterior (occasionally anterior) to common hepatic duct. It always divides into anterior branch supplying segments V and VIII, and posterior branch supplying segment IV and V. The anterior division often supplies a branch to segment I and the gallbladder (Standring et al 2008)

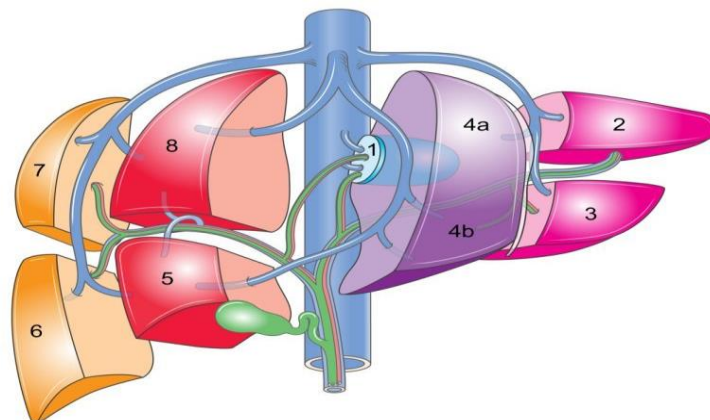


Figure 2.1 shows the liver segments (Standring et al 2008)

The portal vein begins at the level of the second lumbar vertebra. It formed by convergence of superior mesenteric and splenic veins. It lies anterior to the inferior vena cava (IVC) and posterior to the neck of the pancreas. It lies obliquely to the right and ascends behind the first part of duodenum, the common bile duct and gastroduodenal artery. At this point it is directly anterior to the inferior vena cava. It enters the right border of the lesser omentum, and ascends anterior to the epiploic foramen to reach the right end of the porta hepatic. It then divides into right and left main branches, which accompany the corresponding branches of the hepatic artery

Into the liver. (Standring et al. 2008).

The hepatic veins lie in the planes that divide the lobes and segments of the liver. Thus, they are intersegmental and drain parts of adjacent segments. The hepatic veins arise as central veins of the liver lobules. They coalesce to form interlobular veins, several orders of collecting veins, and right, middle, and left hepatic veins that emerge from the liver to enter the inferior vena cava. (Skandalaki.et al 2008).

Lymph from the liver has abundant protein content. Lymphatic drainage from the liver is wide and may pass to nodes both above and below the diaphragm. (Standring et al. 2008).

#### **2.1.4: Intra hepatic bile ducts (IHBD)**

There are more than 2 km of bile ductless and ducts in the adult human liver (Fig. 2.2). These structures are far from being inner channels, and are capable of significantly modifying biliary flow and composition in response to hormonal secretion. Bile secretion starts at the level of the bile canaliculi, the smallest branch of the biliary tree. (Pierre and Laille 2014)

The bile canaliculi join to form ductless (canals of Herring) which lined with cuboidal epithelial cells. These are not hepatocytes and have a complete basal

lamina, the ductless open into interlobular bile ducts, which form part of the portal triads. The interlobular ducts join to form right and left lobar ducts, which join at the hilum to form extrahepatic common hepatic duct. The interlobular bile ducts, form a richly anastomosing network that closely surrounds the branches of portal vein. These ducts increase in caliber and possess smooth muscle fibers within their wall as they reach the hilus of the liver. Furthermore, as they become larger, the epithelium becomes increasingly thicker and contains many elastic fibers. These ducts anastomose to form the segmental branches (from segment I to segment VIII) (Pierre and Laillie 2014),

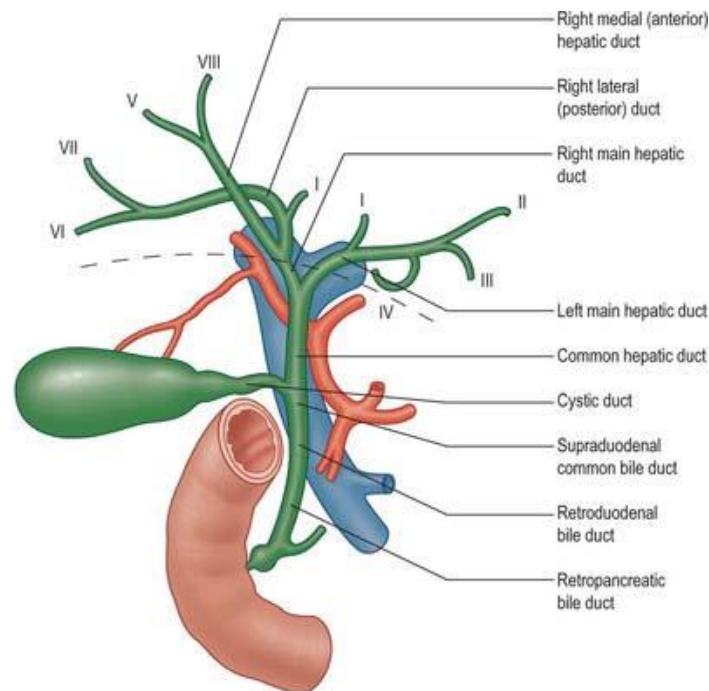


**Figure 2.2** shows the intrahepatic bile ducts(Standring et al 2008)

### **Left biliary tree**

The left hemi liver, segmental branches from segment (II) and segment (III) anastomose to form left hepatic duct in the region of the umbilical fissure. The anastomosis of segment (IV) to the left hepatic duct usually occurs as a single

trunk to the right of the umbilical Fissure in 67% of individuals. (Pierre and Laillie 2014)

Variation of the intrahepatic bile ducts: As illustrated previously, the incidence of right anterior and posterior sectorial ducts joints to form the right hepatic duct occurs in only 57% of people (Pierre and Laillie 2014). In 12%, the right anterior and right posterior ducts join at the junction with the left hepatic duct without the existence of the right hepatic duct. In 20% of cases, drainage occurs directly into the common hepatic duct. There was variation in the segmental anastomosis in the right liver. The main right segmental

Drainage was variable in 9% of segment V, 14% in segment VI, and 29% in segment VII. The Variation in segment VII not reported. (Pierre and Laillie 2014). (Skandalaki.et al 2008).

The left hepatic duct usually forms by confluence of the ducts that drain medial and lateral segments. With regard to left liver, 67% of individuals have previously described their anatomy. The main variation lies in the ectopic drainage of segment IV It reported that 2% drain directly into the common hepatic duct, and 27% drain directly into segment II or segment III only. (Skandalaki.et al 2008)

Another form of ectopic drainage of the intrahepatic ducts is involvement of the cystic ducts and the gallbladder. As illustrated, these variations are important to note (Pierre and Laillie 2014).

The confluence takes place at the right of the hilus of the liver, anterior to the portal venous bifurcation and overlying the origin of the right branch of the portal vein (Fig. 2.3). The biliary confluence separated from the posterior aspect of segment IV of the left liver by the hilar plate, which is the fusion of connective tissue enclosing the biliary and vascular structures with Glisson's capsule (Pierre and Laillie 2014). The classic junction occurs in 61% of instances. During a right hepatectomy, the anatomical situation of the main biliary confluence explains the

risk of ligating the confluence or the left duct. The Bismuth–Corlette classification is valid only for a normal confluence. In the event of biliary abnormality, it is necessary to take into account not only the type of confluence, but also its height in relation to the portal vein. Skandalaki.et al (2008).

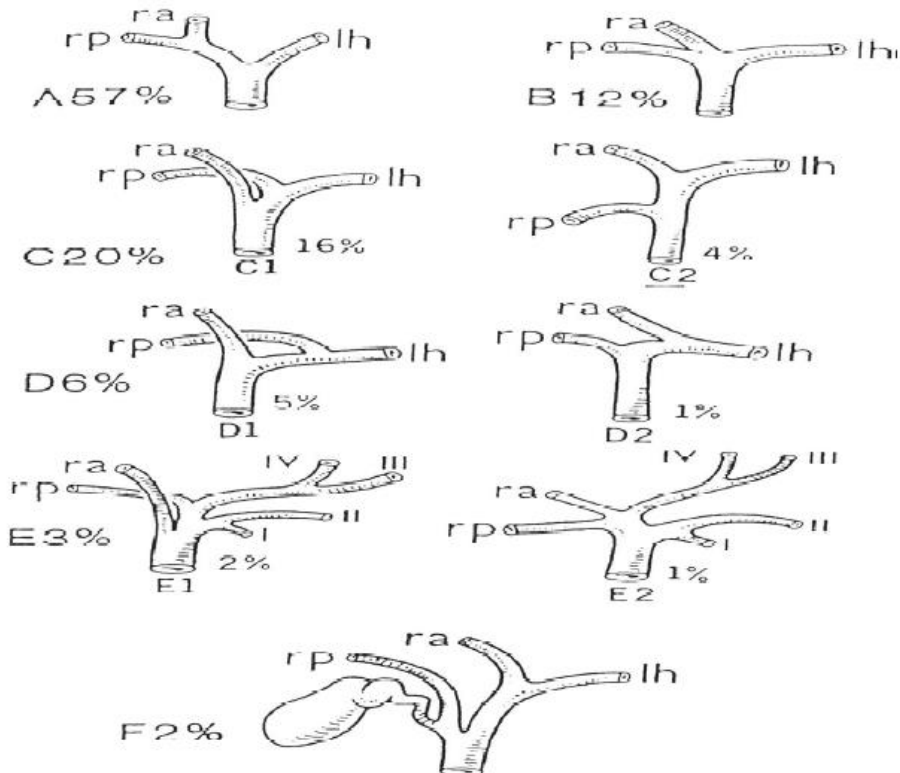


**Figure 2.3** shows the biliary confluence (Standring et al 2008)

### 2.1.5 Extrahepatic biliary duct

The extrahepatic biliary tree consists of right and left hepatic ducts, common hepatic duct, cystic duct, gallbladder and common bile duct. (Standring et al. 2008).

The main right and left hepatic ducts emerge from the liver and unite near to right end of the porta hepatic as the common hepatic ducts begin. The common hepatic duct formed by the union of the right and left hepatic ducts in the porta at the

transverse fissure of the liver. Its lower end defined as its junction with the cystic duct. The distance between these points varies from 1.0 cm to 7.5 cm. The diameter of the duct is about 0.4 cm Skandalaki.et al (2008). This descends and joins on its right at an acute angle by the cystic duct to form the common bile duct. The common Hepatic duct lies to the right of the hepatic artery and anterior to the portal vein in free edge of lesser omentum. (Standring et al. 2008)

The cystic duct drains the gallbladder into the common bile duct. It between 3 & 4 cm long, passes posteriorly to the left from the neck of the gallbladder, and joins the common hepatic duct to form the common bile duct. It usually runs parallel to, and is adherent to the common hepatic duct for a short distance before joining it. The junction usually occurs near porta hepatic but may be lower down in the free edge of the lesser omentum. (Standring et al. 2008).

The cystic duct contains a series of 5 to 12 crescent-shaped folds of mucosa similar to those seen in the neck of the gallbladder. These form the so-called spiral valve of Heister. The length of the cystic duct and the manner in which it joins the common hepatic duct vary. The cystic duct joins the hepatic duct at an angle of about 40° in 64-75% of individuals. In 17-23%. The cystic duct parallels the hepatic duct for a longer or shorter distance and may even enter the duodenum separately. This has been call "absence" of the common bile duct (Skandalaki.et al 2008).

The gallbladder is a flask-shaped, blind-ending diverticulum attached to the common bile duct by the cystic duct it is 7-10 cm long and has a capacity of 30-50 ml. (Skandalaki .et al 2008). It usually lies in a shallow fossa in the liver parenchyma covered by peritoneum continued from the liver surface. This attachment can vary widely. At one extreme the gallbladder may be almost completely buried within the liver surface, having no peritoneal covering (intraparenchymal pattern); at the other extreme it may hang from a short mesentery formed by the two layers of

peritoneum separated only by connective tissue and a few small vessels (mesenteric pattern). The gallbladder divided into a fundus, body, infundibulum, and neck (Standring et al. 2008).

The fundus is usually located at the angle of the ninth costal cartilage with the right border of the rectus sheath and to the left of the hepatic flexure of the colon. It has been completely covered by peritoneum, because it projects beyond the lower border of the liver (Skandalaki et al 2008).

The body of the gallbladder is in contact with the first and second portions of the duodenum and occupies the gallbladder fossa of the liver. The body also related to the transverse colon. (Standring et al. 2008).

The infundibulum is the angulated posterior portion of the body between the neck and the point of entrance of the cystic artery. When this portion dilated, with eccentric bulging of its medial aspect, it called a Hartmann's pouch (Skandalaki et al 2008).

The neck lies at the medial end close to the porta hepatic, and usually has a short peritoneal covered attachment to the liver (mesentery); this mesentery usually contains the cystic artery. The mucosa at the medial end of the neck obliquely ridged, forming a spiral groove continuous with the spiral valve of the cystic duct. (Standring et al. 2008).

The duct of Luschka is a small bile duct, running in the bed of the gallbladder, outside the wall. It is present in 50% of individuals (Pierre and Laille 2014).

The common bile duct begins at the union of the cystic and common hepatic ducts and ends at the papilla of Vater in the second part of the duodenum. It varies in length from 5 cm to 15 cm, depending on the actual position of the ductal union. In 22%, the common hepatic and cystic ducts on average, run parallel for 17 mm before the ducts actually unite. The average diameter is about six mm (Skandalaki et al 2008).



It descends posteriorly and slightly to the left, anterior to the epiploic foramen, in the right border of the lesser omentum. It lies anterior and to the right of the portal vein and to the right of the hepatic artery. It passes behind the first part of the duodenum with the gastroduodenal artery on its left, and then runs in a groove on the super lateral part of the posterior surface of the head of the pancreas. It lies anterior to the inferior vena cava and sometimes embedded in the pancreatic tissue. The duct may lie close to the medial wall of the second part of the duodenum or as much as 2 cm from it. Even when it has been embedding in the pancreas, a groove in the gland marking its position palpated behind the second part of the duodenum (Standring et al. 2008).

Hepatopancreatic ampulla (of Vater)it lies medial to the second part of the duodenum; the common bile duct approaches the right end of the pancreatic duct. The ducts enter the duodenal wall together, and usually unite to form the hepatopancreatic ampulla. Rarely the common bile duct and pancreatic duct drain into the duodenum separately. (Skandalaki. et al 2008).

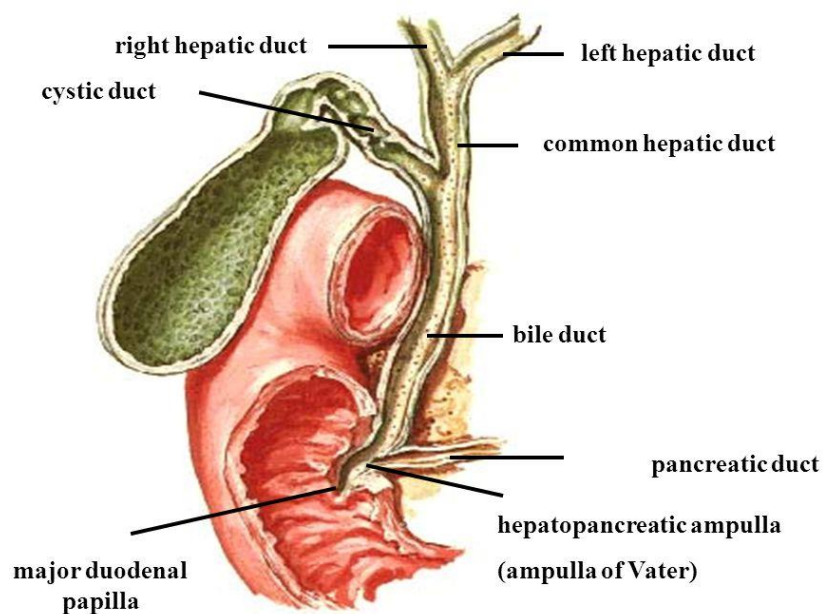


**Figure 2.4** the anatomy of the extrahepatic biliary system(Skandalaki. et al 2008).

### **2.1.5.1: Vascular supply and lymphatic drain:**

The cystic artery: usually arises from the right hepatic artery. It usually passes posterior to the common hepatic duct and anterior to the cystic duct to reach the superior aspect of the neck of the gallbladder (fig1.4). It divides into superficial and deep branches. The superficial branch ramifies on the inferior aspect of the gallbladder body, the deep branch on the superior aspect. These arteries anastomose over the surface of the body and fundus. (Standring et al. 2008).

Cystic vein: The venous drainage of the gallbladder is rarely by a single cystic vein. There are usually multiple small veins (fig2.4). Those arising from the superior surface of the body and neck lie in areolar tissue between the gallbladder and liver and enter the liver parenchyma to drain into the segmental portal veins. (Standring et al. 2008).

Lymphatic drain: Long collecting trunks drain the lymphatic plexus of the fundus and body of the gallbladder. The trunks are on the right, left borders (lateral and medial borders of the gallbladder wall), and connected by an oblique trunk to form a large "N" on the surface. The trunks are on the left drain into cystic node, which lies in the angle formed by the cystic and common hepatic ducts. The trunks on the right follow the cystic duct, passing without entering the cystic node. These vessels and the efferent vessels of the cystic node drain to the node of the anterior border of the epiploic foramen, and to the superior pancreaticoduodenal nodes on the common bile duct. (Skandalaki. et al 2008).

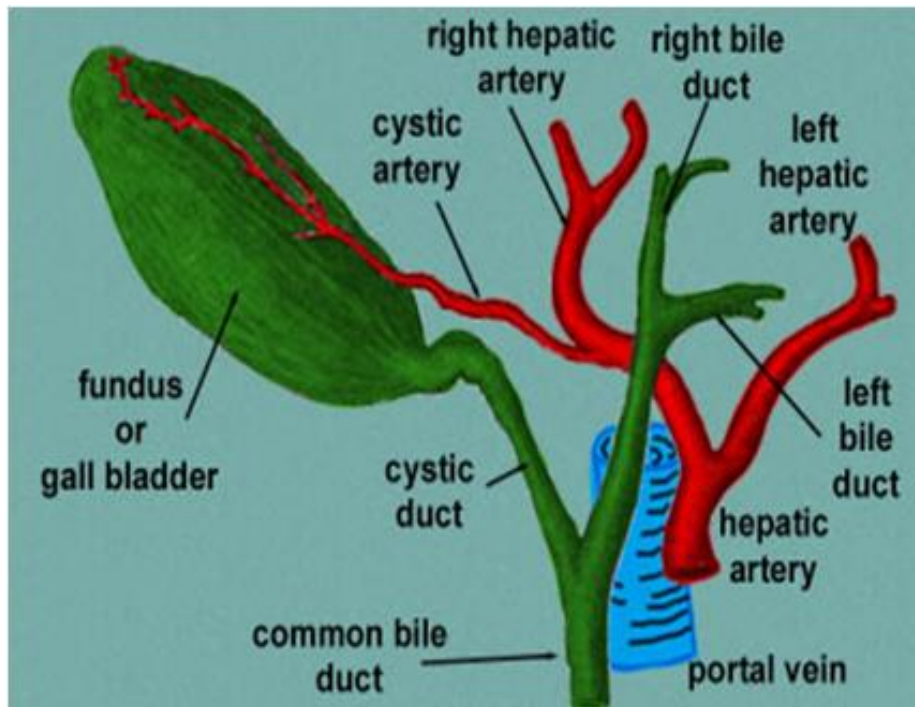


Figure 2.5: Blood supply to the extrahepatic bile ducts. (Skandalaki. et al 2008).

### 2.1.6: The pancreas:

The pancreas is the largest digestive glands and performs a range of both endocrine and exocrine functions. The pancreas is salmon pink in color with a firm, lobulated smooth surface. The pancreas divided into four parts: head, neck, body, and tail. (Standring et al. 2008).

The pancreas lies transversely in the retroperitoneal sac, between the duodenum on the right and the spleen on the left. It related to the omental bursa above, the transverse mesocolon anteriorly, and the greater sac below. For all practical purposes, the pancreas is a fixed organ. (Skandalaki. et al 2008).

The head of the pancreas lies to the right of the midline, anterior and to the right side of the vertebral column. (Standring et al. 2008) It flattened and has an anterior and posterior surface. The anterior surface is adjacent to pylorus and transverse colon. The posterior pancreaticoduodenal vascular arcade is a major entity on the posterior surface of the head. (Skandalaki. Et al 2008).

The neck of the pancreas is only 0.2 cm wide, it links head and body. It is often the anterior portion of the gland. (Standring et al. 2008).

The body of the pancreas runs from the left side of the neck to the tail. It is the longest portion of the gland and becomes progressively thinner and less broad towards the tail. It is triangular in cross-section and described as having three surfaces: anterosuperior, posterior, and anteroinferior. (Standring et al. 2008).

The tail of the pancreas is the narrowest, most lateral portion of the gland and lies between the layers of the splenorenal ligament. It is continuous medially with the body and is between 1.5 and 3.5 cm long in adults. (Standring et al. 2008).

The exocrine pancreatic tissue drains into multiple small lobular ducts, which drain into a single main duct (Skandalaki. et al 2008).

The main pancreatic duct runs within the substances of the gland from left to right. It tends to lie towards the posterior more than anterior surface. The junction of several lobular ducts in the tail forms the main pancreatic duct. As it runs within the body it increases in caliber as it receives further lobular ducts, which join it almost at right angles to the axis of the main duct to form a 'herringbone pattern'. On ultrasound the duct can often be demonstrated, measuring 3 mm in diameter in the head, 2 mm in the body, and 1 mm in the tail in adults. As it reaches the neck of the gland it usually turns inferiorly and posteriorly towards the bile duct, which lies on its right side. These two ducts enter the wall of the descending part of the duodenum

Obliquely and unite in a short dilated hepatopancreatic ampulla (Standring et al. 2008).

#### **2.1.6.1 Blood supply:**

The pancreas has rich arterial supply derived from the coeliac axis and superior mesenteric arteries via both named vessels and multiple small unnamed vessels. (Skandalaki. et al 2008).

**Inferior pancreaticoduodenal artery:**The inferior pancreaticoduodenal artery arises from the superior mesenteric artery or its first jejunal branch, near the superior border of the third part of the duodenum. (Skandalaki. et al 2008)

**Superior pancreaticoduodenal artery:**The superior pancreaticoduodenal artery is usually double. The anterior artery is a terminal branch of the gastroduodenal artery. It supplies branches to the head of the pancreas. The posterior artery is usually a separate branch of the gastroduodenal artery arising at the upper border of the first part of the duodenum. The posterior superior artery supplies branches to the head of the pancreas and the first and second parts of the duodenum. (Standring et al. 2008).

**Venous drainage:**The venous drainage of the pancreas is primarily into portal system. The head and neck drain primarily via superior and inferior pancreaticoduodenal veins. The body and tail drain mostly via small veins running directly into the splenic vein along the posterior aspect of the gland or occasionally directly into the portal vein. Small venous channels exist between the gland and the retroperitoneal veins, draining into the lumbar veins and these may hypertrophy and become clinically significant in cases of portal hypertension. (Standring et al. 2008).

**Lymphatic drainage:**As the position of the pancreas might predict, lymphatic drainage is centrifugal to the surrounding nodes. The lymphatic vessels of the pancreas arise in a rich, per lobular, and interanastomosing network. Channels course along the surface of the gland and in the interlobular spaces with the blood vessels. These lymphatic drains into five main collecting trunks and five lymph node groups: superior nodes, inferior nodes, anterior nodes, posterior nodes, and splenic nodes (Skandalaki. et al 2008).

### **2.1.2: Physiologic Anatomy of Biliary Secretion:**

Bile fulfils two major functions. It participates in the absorption of fat and forms the vehicle for excretion of cholesterol bilirubin, iron, and copper. Bile acids are the main active component of biliary secretion, then secreted into the duodenum, and efficiently reabsorbed from the terminal ileum by the portal venous system (Standring et al. 2008).

Bile secreted in two stages by the liver: the initial portion secreted by the principal functional cells of the liver, hepatocytes; this initial secretion contains large amounts of bile acids, cholesterol, and other organic constituents. It secreted into minute bile canaliculi that originate between the hepatic cells. Next, the bile flows in the canaliculi toward the interlobular septa, where the canaliculi empty into terminal bile ducts and then into progressively larger ducts, finally reaching the hepatic duct and common bile duct. From these, either the bile empties directly into the duodenum or diverted through the cystic duct into the gallbladder, a second portion of liver secretion added to the initial bile. This additional secretion is a watery solution of sodium and bicarbonate ions secreted by epithelial cells that line the ductless and ducts. This second secretion sometimes increases the total quantity of bile by as much as an additional 100 percent. The second secretion stimulated especially by secretin, which causes release of additional quantities of bicarbonate ions to supplement the bicarbonate ions in pancreatic secretion (for neutralizing acid that empties into the duodenum from the stomach (Skandalaki. et al 2008)

### **2.1.3: Pathology of the liver, biliary system, and pancreas:**

The liver and its companion: biliary ducts and gallbladder considered together because of their anatomic proximity, their interrelated functions, and the overlapping features of some of the diseases that affect these organs (Skandalaki. et al 2008).

The liver is vulnerable to a wide variety of metabolic, toxic, microbial, circulatory, and neoplastic insults. The dominant primary diseases of the liver are viral hepatitis, alcoholic liver disease, and hepatocellular carcinoma. More often, hepatic damage is secondary, to some of the most common diseases in humans, such as cardiac decompensation, disseminated cancer, and extrahepatic infections. (Kumar et al.2004)

### **2.1.3.1 The Liver:**

The liver is almost inevitably involved in blood-borne infections, whether systemic or arising within the abdomen. The foremost hepatic infections are viral in origin. Other infections in which the hepatic lesion is prominent include miliary tuberculosis, malaria, staphylococcal bacteremia, the salmonellosis, candida, and amebiasis (Skandalaki. et al 2008).

**Viral hepatitis:**The term viral hepatitis reserved for infection of the liver caused by a group of viruses having a particular affinity for the liver. Systemic viral infections that can involve the liver include.

Infectious mononucleosis (Epstein-Barr virus), which may cause a mild hepatitis during the acute phase,

Cytomegalovirus, which particularly found in the newborn or immunosuppressed patient.

Yellow fever, which considered as the major and serious cause of hepatitis in tropical countries. (Kumar et al.2004).

The radiological feature of viral hepatitis: The US finding in acute viral hepatitis includes "Starry-sky" appearance: Echogenicity of portal venous walls Hepatomegaly &periportallucency edema (Federle, 2004).

The MR Findings in Viral hepatitis **are** increase in T1 & T2 relaxation times of liver. And in T2WI show High signal intensity bands paralleling portal Vessels

(periportal edema). Alcoholic steatohepatitis (diffuse fatty infiltration), in T1WI while in-phase GRE image show Increased signal intensity of liver than spleen or muscle in T1WI out-of-phase GRE image Decreased signal intensity of liver (due to lipid in liver) (Federle, 2004).

**Pyogenic Liver Abscesses:** Liver abscesses result from parasitic infections, the parasitic liver abscesses or bacterial abscesses are more common, representing a complication of an infection elsewhere (Kumar et al. 2004). Most common causes of pyogenic abscess are Diverticulitis, Ascending cholangitis Infection from infarcted tissue (e.g., post liver transplantation, necrotic tumor) (Federle, 2004).

The Simple pyogenic abscess chest x ray show Elevation of right hemi diaphragm & Right lower lobe atelectasis .the Plain x-ray abdomen show Hepatomegaly, intrahepatic gas, air-fluid level (Federle 2004).

The Simple pyogenic abscess demonstrated on non-enhanced CT as Well defined, round, hypodense mass. Otherwise, in contrast enhanced CT demonstrated as sharply defined, round, hypodense mass with Rim- or capsule- and septal-enhancement and Right lower lobe atelectasis & pleural effusion (Federle, 2004)

The MR Findings of Simple pyogenic abscess in T1WI appear Hypointense, on T2WI appear as hyper intense mass with high signal intensity on the perilesional edema, and In contrast enhanced T1 weighted image demonstrated as Hypointense mass. The MRCP is highly specific in detecting Obstructive biliary pathology the Leading cause of cholangitis, pyogenic abscess. (Federle 2004)

**Liver cirrhosis:** Chronic liver disease characterized by diffuse parenchymal necrosis with extensive fibrosis & regenerative nodule formation (Federle 2004).

The Classification of cirrhosis based on morphology, histopathology, & etiology as: Micro nodular (Laennec) cirrhosis, Alcoholism Macro nodular (post necrotic) cirrhosis: Viral hepatitis & Mixed cirrhosis (Kumar et al 2004).



The MR Findings in liver cirrhosis include Siderotic regenerative nodules: Paramagnetic effect of iron within nodules. In T1WI: Hypointense, in T2WI: Increased conspicuity of low signal intensity T2 Gradient-echo & fast low-angle shot (FLASH) images markedly appear hypo intense. (Federle 2004).

### **2.1.3.2: Intrahepatic biliary systems:**

**Primary Biliary Cirrhosis:**Primary biliary cirrhosis is a chronic, progressive, and often fatal cholesteric liver disease, characterized by the destruction of intrahepatic bile ducts, portal inflammation, and scarring, and the eventual development of cirrhosis and liver failure (Kumar et al .2004).

**Secondary biliary cirrhosis:** Prolonged obstruction of the extrahepatic biliary tree results in profound alteration of the liver itself. The most common cause of obstruction in adults is extra hepatic cholelithiasis followed by malignancies of the biliary tree or head of the pancreas (Kumar et al .2004).

**Primary sclerosing cholangitis:**Primary sclerosing cholangitis characterized by inflammation and obliterative fibrosis of intrahepatic and extrahepatic bile duct, with dilation of preserved segments. Primary sclerosing cholangitis commonly found in association with inflammatory bowel disease, particularly chronic ulcerative colitis (Kumar et al 2004).

**Cairoli disease:** The larger ducts of the intrahepatic biliary duct are segmentally dilated and may contain inspissated bile. Pure forms are rare; this disease is usually associated with portal tract fibrosis of the congenital hepatic fibrosis (Kumar et al .2004). The Radiographic Findings of caroli disease on the (ERCP) appear as:Saccular dilatations of IHBDs, stones, strictures also May show communicating hepatic abscesses. The non-enhanced CT show Multiple, rounded, hypodense areas inseparable from dilated IHBD and contrast enhanced CT show Enhancing tiny dots (portal radicles) within dilated IHBD. On MR Carolidisease appear in T1 WI as Multiple, small, hypo intense, saccular dilatations of IHBD, while in

T2WI appear as Hyper intense and in T1 with contrast as Enhancement of portal radicles within dilated IHBD. The (MRCP) show Multiple hyper intense oval-shaped structures and

Luminal contents of bile ducts appear hyper intense in contrast to portal vein, which appears as signal void (Federle 2004).

### **2.1.3.3: extrahepatic biliary system:**

**Cholelithiasis (gallstone):** There are two main types of gallstones. In the West, about 80% are cholesterol stones, containing more than 50% of crystalline cholesterol monohydrate. The remainder is composed predominantly of bilirubin calcium salts and is designated pigment stones (Kumar et al .2004).

**Choledocholithiasis:** Choledocholithiasis is stones or calculi Located in Intra- & Extrahepatic bile ducts (more common in CBD). Its Size range Varies from 1-15 mm. Choledocholithiasis is the most frequent cause of biliary obstruction without ductal dilatation (Kumar et al .2004).

**Choledocholithiasis Findings on non-enhanced CT** show Attenuation of calculi varies from less than water density, through soft tissue, to dense calcification, "Bull's eye" sign: Rim of bile surrounding a stone within duct and thin meniscus of water density bile around stone posteriorly The MR Findings on MRCP, Bile appear Very bright signal and Ductal stones appear as Decreased signal intensity foci. (Federle 2004).

**Mirizzi syndrome:** It is Partial or complete obstruction of common hepatic duct due to gallstone impacted in cystic duct or infundibulum of gallbladder Mirizzi syndrome appear on the ERCP as Extrinsic narrowing of common hepatic duct; dilated intrahepatic ducts; lack of GB filling defects. And on MRCP, demonstrated as dilated intrahepatic ducts, filling defect in common hepatic duct (Federle 2004).

**Cholecystitis:** Is Inflammation of gallbladder may be acute, chronic, or acute superimposed on chronic. The acute cholecystitis either calculous cholecystitis or

non calculous cholecystitis (Kumar et al .2004). The Radiographic Findings in ERCP: document common bile duct, (CBD) stones with associated cholangitis, and No filling of gallbladder. The non-enhanced CT shows Distended GB with Edematous pericholecystic fat with stranding & calcified gallstones the contrast enhanced CT show uncomplicated cholecystitis, GB wall thickening & increased mural enhancement (Federle 2004).

The MR Findings in T2WI as Distended GB with stones & High signal pericholecystic fat. In contrast enhanced T1 as “Rim sign” of increased hepatic enhancement in patient with gangrenous cholecystitis and Focal interruption of enhancement (Federle 2004).

**Biliary atresia:** Biliary atresia defined as a complete obstruction of lumen of the extrahepatic biliary tree within the first 3 months of life. It is the single most frequent cause of death from liver disease in early childhood (Kumar et al .2004)

**Choledochal cysts:** Choledochal cysts are congenital dilations of common bile duct, presenting most often in children before age 10 with the non specific symptoms of jaundice and/or recurrent abdominal pain that are typical of biliary colic. Choledochal cysts predispose to stone formation, stenosis and stricture, pancreatitis, and obstructive biliary complications within the liver. In elder patient, the risk of bile duct carcinoma elevated (Kumar et al .2004).

In Radiography of upper gastrointestinal series Choledochal cysts demonstrated as anterior displacement of second part of Duodenum & antrum, and inferior displacement of duodenum and Widening of duodenal sweep.

The ERCP Demonstrates all types of choledochal cysts such as Cystic or fusiform dilatation of common duct and also Shows mucosal diaphragm & aberrant insertion of CBD into pancreatic duct.

On MR in T1 WI the Choledochal, cysts appear Hypointense, in T2WI as Hyperintense, and in MRCP the Bile appears hyper intense in contrast to portal vein (Federle 2004).

**Carcinoma of the gallbladder:** Carcinoma of the gallbladder slightly more common in women and occurs most frequently in the seventh decade of life. Gallstones present in 60% to 90% of cases. In Asia, where pyogenic and parasitic diseases of the biliary tree are common, the coexistence of gallstones is much lower. Presumably, gall bladders containing stones or infectious agents develop cancer because of irritative trauma and chronic inflammation (Kumar et al .2004).

**Carcinomas of the extrahepatic biliary tree:** Carcinomas of the extrahepatic biliary ducts, down to level of the ampulla of Vater, are uncommon tumors. They are extremely insidious tumors and generally produce painless, progressively deepening jaundice (Kumar et al.2004).

#### **2.1.3.4: The pancreas:**

**Pancreatitis:** Pancreatitis encompasses a group of disorders characterized by inflammation of the pancreas. It may be acute or chronic. An acute pancreatitis is a group of reversible lesions characterized by inflammation of the pancreas ranging in severity from edema and fat necrosis to parenchymal necrosis with severe hemorrhage. (Kumar et al 2004).

Chronic pancreatitis is characterized by inflammation of the pancreas with destruction of exocrine parenchyma, fibrosis, in the late stages, although chronic pancreatitis may present as repeated bouts of acute pancreatitis, the chief distinction between acute and chronic pancreatitis is the irreversible impairment in pancreatic function that is characteristic of chronic pancreatitis (Kumar et al 2004)

**Non-Neoplastic Cysts:** A variety of cysts can arise in the pancreas. Most are non-neoplastic pseudocysts, but congenital cysts and neoplastic cystic tumors also

occur. In general, unilocular cysts tend to be benign, while multilocular cysts are more often neoplastic and possibly malignant (Kumar et al .2004)

Cystic Neoplasm:Cystic neoplasm makes up fewer than 5% of all pancreatic neoplasm. While some, such as the serous cyst adenoma, are entirely benign, others, such as mucinous cystic neoplasm, can be benign, borderline malignant, or malignant. (Kumar et al .2004)

#### **2.1.4: MRCP physic& equipment:**

The basic principle of MRI depends on the fact that the nuclei of certain elements align with the magnetic force when placed in a strong magnetic field. At the field strengths currently used in medical imaging, hydrogen nuclei (protons) in water molecules and lipids are responsible of producing images. If a radiofrequency pulse at an appropriate frequency (resonant frequency) is applied, a proportion of the protons changes alignment, flipping through a rest angle, and rotate in phase with one another. Following this radiofrequency pulse, the protons return to their original positions. As the protons realign (relax) they induce a radio signal which, although very weak, can be detected and localized by coils placed around the patient. An image representing the distribution of the strength of the hydrogen built up, T1 and T2; T1 depends on the time the protons take to return to the axis of the diphas. A T1-weighted image is one in which contrast between tissues is due mainly to their T1 relaxation properties, while in a T2-weighted image the contrast is due the T2 relaxation properties. Some sequence produce mixed (often called; balanced') images which approximate to T1 and T2 relaxation times and these processes therefore appear lower in signal (blacker) on a T1-weighted scan and higher in signal (whiter) on a T2 weighted scan than the normal surrounding tissues. The T1 and T2 weighting of an image can be selected by appropriately altering the timing and sequence of radiofrequency pulses. (Peter Armstrong Martin L.wastie et Al).

A typical MRI scanner consists of a large circular magnet. Inside the magnet are the radiofrequency transmitter and receiver coils, as well as gradient coils to allow spatial localization of the MRI signal. Ancillary equipment converts the radio signal into a digital form by a computer to form a final image. (Peter Armstrong Martin L.wastie et al)

### **2.1.5 MRCP technique:**

MR imaging uses a powerful magnetic field, radio waves, and a computer to produce detailed pictures of organs, soft tissues, bone, and virtually all other internal body structures. The Contraindications of MRI abdomen are Patients with cardiac pacemakers, or neuro-stimulators cannot have MRI. Additionally Patients with pins, plates, screws, and joint replacements can have an MRI as long as it has been 6 weeks since placement of the device. Patients with stents and filters can have an MRI as long as it has been at least 6-8 weeks since placement of the device. (Dahlstrom. 2009).

MRCP Originally described in 1991, takes advantage of the inherent contrast-related properties of fluid in the biliary and pancreatic ducts. (Fulcher. 1999).

The basic principle underlying MRCP is that Images of fluid-containing organs could obtain using MR imaging sequences based on the long T2relaxation time of static fluids. On heavily T2-weighted, images (echo times longer than 150 MS), these fluids exhibit high signal intensity, and where as the signal of surrounding body organs and tissues markedly suppressed (Maccioni et al 2010) Since a large component of residual background signal in the abdomen arises from fat, magnetic Resonance techniques that allow the selective suppression of fat can substantially reduce the background signal. (Sanyal. et al 2012). Contrast agents are not strictly necessary to obtain MRCP images. However, negative oral contrast agents (so called “super paramagnetic” agents) usefully employed to reduce the brightness of

the gastric and intestinal fluids, in order to enhance the evidence and brightness of the biliary tree and pancreatic ducts. (Sanyal et al 2012).

Heavily T2-weighted images originally achieved using a gradient-echo (GRE) balanced steady-state free precession technique. A fast spin-echo (FSE) pulse sequence with long echo time (TE) then introduced shortly after. With the advantages of relatively high spatial resolution, a higher signal-to-noise ratio and contrast-to-noise ratio, and therefore, lower sensitivity to motion and susceptibility artifacts. Limitations of SSFSE techniques include image blurring induced by long ETLs, flow artifacts within the biliary tree that can occasionally simulate stones or Masses Alexander.

Modified FSE sequences had been describe, including rapid acquisition with rapid enhancement (RARE), half-Fourier acquisition single-shot turbo spin-echo (HASTE) and fast-recovery fast spin-echo (FRFSE) sequences. Both breath-hold (using a single shot approach) and non-breath-hold techniques (with respiratory triggering) had been used, with images obtained as either a two-dimensional (2D) or three-dimensional (3D) acquisition. (Maccioni et al. 2010).

A 3D technique provides a higher signal to noise ratio, which traded off for thinner contiguous slices. Acquiring images with near isotropic voxels allows improved post-processing manipulation of the images with multi-planar reconstruction, maximum intensity projection (MIP) and volume rendering. (Maccioni et al. 2010)

To ensure that the gall bladder, Hepato-biliary and pancreatic ducts filled with fluid and at their maximum distension, the patient would need to fast. It is recommended that the patient be nil per oral for at least four hours prior to commencing the examination. Throughout this period, the patient is permitted to drink clear fluids only (namely water), and routine medication is allowed as per normal. (Mandaranoet al. 2008)

Mitchell (2007) as cited by Mandarano (2008) concurs that suspended expiration is more consistent, and provides less motion variation, whereas full inspiration reserved for situations where the lung diaphragm needs to be in more inferior position. It is imperative that the patient understands their role and that their cooperation and active participation is needed to ensure overall diagnostic success. If the breath hold technique is not adequate, then the CBD and the main pancreatic duct may not appear to unite or may appear either stenotic or dilated. (Mandarano et al. 2008).

The Coronal T2-weighted images are thin collimation images (3-5 mm), and then processed to obtain a MIP (maximum intensity projection) image, which is a cholangiogram like image. Otherwise a coronal thick slab (30 to 50 mm) obtained, to produce the same effect in a very short time (<5 seconds). Usually both imaging technique are associated and reviewed, to achieve the higher accuracy. (Sanyal et al 2012).

### **2.1.5 MRCP Technique:**

#### **2.1.5.1: Three Planes Localizer:**

Performed at the beginning of the MRCP exam, obtained in three plans (coronal, sagittal, and transverse). This sequence provides low spatial resolution images demonstrating anatomy for orientation purposes.

#### **2.1.5.2: Axial 2D single shot fast spine echo (SSFSE):**

The purpose of this sequence is obtain images of the hepatic ducts, biliary tree, and pancreatic duct in the transverse plane. Fat suppression improves conspicuity of solid lesions and minimizes phase ghosting artifacts from subcutaneous and intraperitoneal fat. (Westbrook et al 2005). The first prescribed slice figure (2.5) should be almost at the most superior aspect of the liver to ensure that the majority of the right and left hepatic ducts are captured. The inferior prescribed slice should



be located into the lumen of the duodenum to ensure that the sphincter of Oddi captured as well as any variation in the location of the union of the pancreatic duct. (Mandarano et al. 2008)

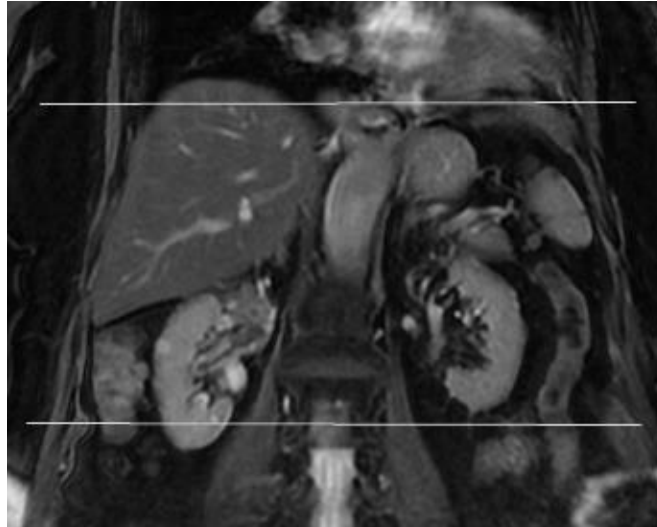
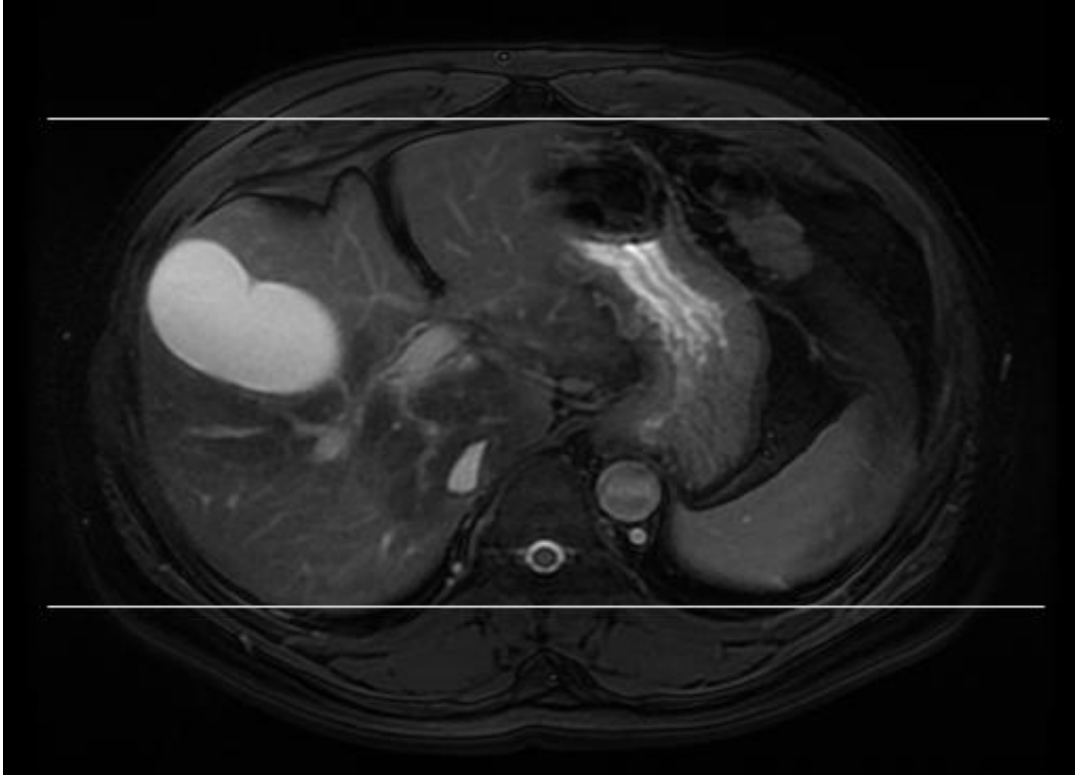


Figure 2.6: Scanning range prescription for the axial 2D SSFSE Fat Suppressed series. (Mandarano et al. 2008)

### **2.1.5.3: Coronal 2D single shot fast spine echo(SSFSE) (Fat Suppressed):**

The reasons for performing this sequence are exactly the same as for the axial series, but another view of the relevant anatomy obtained. In particular, this plane is useful in adding assessment value of the condition of the CBD, cystic duct, hepatic ducts and the gallbladder; with pathology affecting the ampulla of Vater particularly well noted. The scanning range (figure 2.6) should have the prescribed slices commencing within the lumen of the duodenum (to visualize any biliary fluid passing through the sphincter of Oddi) and ending at almost the most anterior surface of the liver (to ensure that the intra hepatic ducts are included).



**Figure 2.7** Scanning range prescription for the Coronal 2D SSFSE Fat Suppressed Sequence in: The diagnostic MRCP examination.(Mandarano et al. 2008)

#### **2.1.5.4: Coronal Oblique three Slabs MRCP:**

The underlying concept is to image fluid within the ducts. And suppressing signal from non-fluid structures. The main aim of this classic MRCP sequence is to demonstrate ductal fluid as hyper intense. While filling defects, such as those caused by stones, displayed as hypo intense. From axial 2D SSFSE images obtain three specific images aimed at the CBD, cystic duct and the pancreatic duct. The first slice straight through the CBD in a coronal fashion the second slice is prescribed parallel to the cystic duct. The third slice needs to prescribe parallel through the pancreatic duct along the head of pancreas, as depicted in figure 2.7 a. b c respectively.



**Figure 2.8A:** the First slice prescribed coronal, directly through the CBD.



**Figure 2.8B:** indicates the second prescribed slice parallel to the cystic duct.

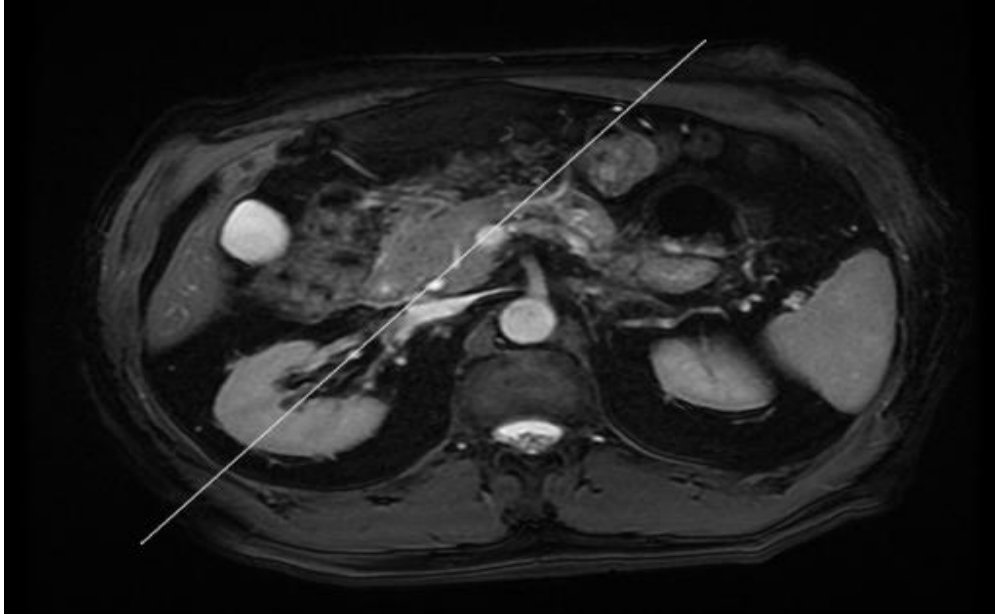
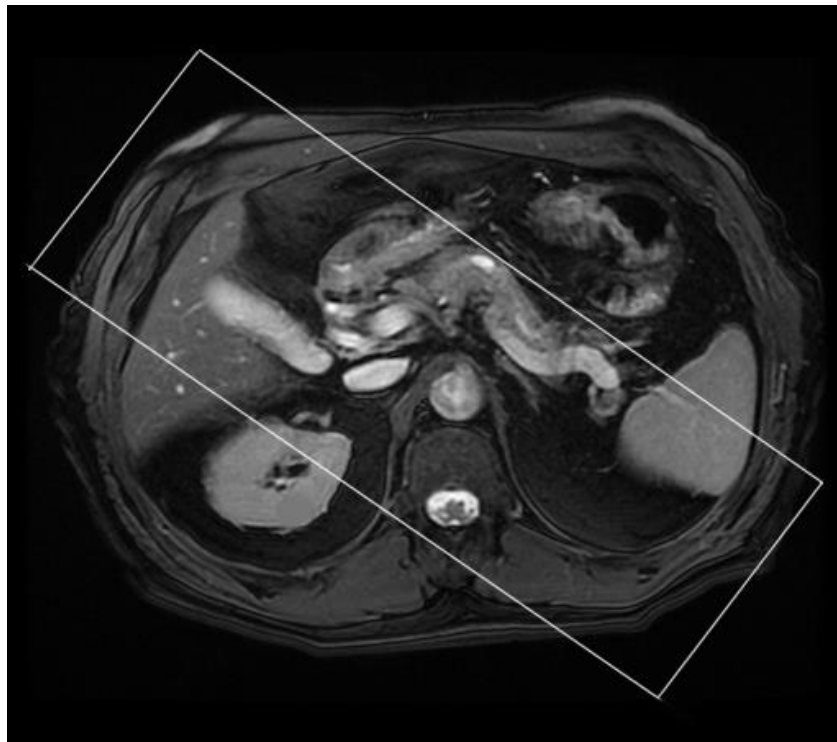


Figure 2.8C: indicates how the third slice prescribed parallel to the main pancreatic duct through the head of pancreas.(Mandarano et al. 2008)

#### **2.1.5.5: Para Coronal 3D MCRP Respiratory Triggered:**

This is also a heavily T2-weighted sequence, but acquired as a 3D volume. The main purpose of this approach is to capture a 3D perspective of the biliary tree, and with appropriate software, permit the observer to rotate the volume representation of the biliary tree in order to view its intricacies from practically limitless angles provides thin, contiguous slices. This volume positioned to capture the entire biliary tree. The Para coronal angle used would be identical to that mentioned in the Coronal Oblique 3D Slab MRCP sequence. The volume centered to and along the cystic duct, and the volume expanded to include the entire components comprising the biliary tree, (Figure 2. 8). It is important to include saturation pulses immediately adjacent to all boundaries of the imaging volume in order to minimize artifacts originating from both respiratory and physiological motion from degrading the data within the imaging volume. (Mandarano et al. 2008)

These source images suitable for further analysis, especially reformatting algorithms such as maximum intensity projection (MIP) and shaded surface display. The frontal MIP reconstruction produces projection images of Pancreatic biliary ductal system that resemble those obtained from directcholangiopancreatography. Furthermore, the data set can be reconstructed in multiple angles (from anteroposterior to lateral views), allowing separation of pertinent structures from overlapping fluid-containing organs. (Soto et al1995)



**Figure 2.9** Volume prescription for the Para-coronal 3D MRCP Respiratory Triggered sequence.(Mandarano et al. 2008)

#### **2.1.5.6: Dynamic Coronal MRCP:**

Offers added possibility of a functional study, during the intravenous administration of secretin, which physiologically stimulates the exocrine pancreas. The secretin rapidly increases the production of pancreatic fluids, thus increasing the duct size and producing an excellent display of the entire pancreatic ductal system (main and secondary ducts). Moreover, by acquiring consecutive MRCP

images every 10 seconds from time 0 to 10 minutes after secretin I.V injection. (0.2 mcg/kg of body weight), it stimulates pancreatic fluid secretion and simultaneously increases the

Oddi sphincter tone for a few minutes, thus producing a mild dilation of the main and secondary ducts. It is possible to evaluate the total amount of increased duodenal fluid, which is a reliable index of the exocrine pancreatic function. In a second phase, the Oddi sphincter relaxes, the pancreatic fluid passes in the duodenal lumen; by quantifying the amount of pancreatic fluids in the duodenum, it is directly assess the pancreatic exocrine function, the so-called cholangiopancreatography quantification

(MRCPQ) (Sanyal et al. 2012).

There is an increasing interest in the use of hepatobiliary contrast agents, such. These agents are hepatocyte-selective T1 weighted MR agents that are administered intravenously and excreted primarily through the biliary system. (Sanyal et al. 2012). The direct visualization of the biliary tree starts after 20 to 100 minutes following injection, according to the different agent, and lasts for 1-2 hours. The use of these contrast agents should provide both anatomic information and functional (Sanyal et al 2012)

On the other hand, (Tschirch et al 2005) as cited by (Hyodo et al 2012) reported that EOB-MRC was sufficient for anatomical visualization of the biliary tree in 40% of patients with liver cirrhosis, and in 100% of adult individuals with normal liver function. The utilization of contrast enhanced -MRC using Gd-EOB-DTPA and the 3D GRE technique is a robust tool that displays the biliary anatomy and provides functional information about physiological or pathological biliary flow. The added diagnostic properties make it invaluable in the accurate detection of bile leaks and cysto-biliary communication (Fulcher et al 1999)

## **2.2 Previous studies:**

Several researches try to determine biliary ductal diameter and ageing effect.

NidhiLal et al 2014 measured diameters of common bile duct in a series of normal Rajasthan population and to measure its correlation with age, sex and anthropometry by using ultrasound. The common bile duct was measured at three locations- at the portal hepatic, in the most distal aspect of head of pancreas and mid-way between these points. Anthropometric measurements including height, weight, and chest circumference, circumference at Tran's pyloric plane, circumference at umbilicus and circumference at hip were obtained using standard procedures.

NidhiLal et al was founded the mean age of study subjects was 34.5 years (Range 18-85 years). Mean diameters of the common bile duct in the three locations were: proximal, 4.0 mm (SD 1.02 mm); middle, 4.1 mm (SD 1.01 mm); and distal, 4.2 mm (SD 1.01 mm) and overall mean for all measures 4.1 mm (SD 1.01 mm). Average diameter ranged from 2.0 mm to 7.9 mm, with 95 percent of the subjects having a diameter of less than 6 mm. We observed a statistically significant relation of common bile duct with age, along with a linear trend. There was no statistically significant difference in common bile duct diameter between male and female subjects. The diameter did not show any statistically significant correlation with any of the anthropometric.

Sakorafas et al (2007) was founded the female gender was associated with higher prevalence, 16% compared to 9% for male. The female gender carried twice the risk of gallstone disease as compared to men, which was especially prominent at a younger age, mainly because of hormonal factors.

Tarig ET al2016 study aimed to measure the normal diameter of the common bile duct and pancreatic duct and correlate this measurement with age and gender.

The study of TARIG et al (2016) for 66 patients 33 male and 33 female their age between 10 to 89 years, they selected randomly when they attended to radiology department for performed MRCP. The diameter common bile duct and pancreatic duct were measured from the 2D images of (SSTSE BH). Then the data analyzed by SPSS to find the mean and standard deviations correlations.

The study found the mean of the diameter common bile duct for female of age groups (30-49) years were ( $5.3\pm 1.2\text{mm}$ ), (50-60) years were ( $5.7\pm 0.8\text{mm}$ ) and (70-89) years were ( $5.3\pm 1.6\text{mm}$ ), and for male of age groups (30-49) years were ( $5.2\pm 1.3\text{mm}$ ), (50-60) years were ( $5.6\pm 0.7\text{mm}$ ) and (70-89) years were ( $5.5\pm 0.6\text{mm}$ ) respectively.

In addition, the study found correlation between the diameter of common bile duct and both male and female were significant of values P 0.017 and P 0.011 respectively

Dig Surg2017 et AL study of Aging has been associated with increasing common bile duct (CBD) diameter and reported as independently predictive of the likelihood of choledocolithiasis. These associations are controversial with uncertain diagnostic utility in patients presenting with symptomatic disease. The current study examined the relationship between age, CBD size, and the diagnostic probability of choledocolithiasis. Methods of study Symptomatic patients undergoing evaluation for suspected choledocolithiasis from January 2008 to February 2011 were reviewed. In the cohort without choledocolithiasis, the relationship between aging and CBD size was examined as a continuous variable and by comparing mean CBD size across stratified age groups. Multivariate analysis examined the relationship between increasing age and diagnostic probability of choledocolithiasis in all patients. Results: Choledocolithiasis was diagnosed by MR cholangiopancreatography (MRCP) or endoscopic retrograde



(ERCP) in 496 of 1,000 patients reviewed. Mean CBD was 6.0 mm ( $\pm 2.8$  mm) in the 504 of 1,000 patients without choledocolithiasis on ERCP/MRCP. Increasing age had no correlation with CBD size as a continuous variable ( $r^2 = 0.011$ ,  $p = 0.811$ ). No difference occurred across age groups (Kruskal-Wallis,  $p = 0.157$ ). Age had no association with diagnostic likelihood of choledocolithiasis (AOR [95% CI] 0.99 [0.98-1.01], adjusted- $p = 0.335$ ). Conclusion of study In a large population undergoing investigation for biliary disease, increasing age was neither associated with increasing CBD diameter nor predictive of the likelihood of choledocolithiasis.

**Chapter three**  
**Materials and methods**

## Chapter three

### Materials and methods

#### 3.1 Materials:

##### 3.1.1 patient:

MRI scans of 55 patients (16 male and 39 female) are used to measure the common bile duct and pancreatic duct. The age of patients ranged from (21 to 78) years.

The data used in this study was collected from two hospitals in Khartoum state: al-Moalem Medical city, Royal Scan Diagnostic Center

The data collected from March 2018 to April 2018.

##### 3.1.2 MRI Machine:

Two MRI machines were used to collect data during this study. This machine was installed in two radiological departments.

Treashing medical city by manufacture Toshiba, installed in 2010 by magnet strength 1.5T.

Royal scan diagnostic center by manufacture by Toshiba, installation in 2012 by magnetic strength 1.5T

#### 3.2 Methods:

##### 3.2.1 Technique used:

Patients were required to fast for 12 hours prior to MR examination. All MRCPs were performed by a 1.5T MR machine (Toshiba) with 120 mT/m maximum gradient capability and phase array body coil. After localizing images, the coronal and axial abdominal images were obtained using T2-weighted pulse sequences. Axial images of the biliary and pancreatic ducts were obtained using T2-weighted

fat suppressed pulse sequence. Both groups' MRCP included breath-hold thick slab single-shot turbo spin echo (SSTSE BH) sequence images.

The parameters of the SSTSE BH sequence were as follows: TR, 3137ms; effective TE, 512 MS; turbo factor, 128; flip angle, 90°; slice thickness, 30 to 40 mm; field of view, 250 mm; matrix, 256 × 205; acquisition time, 8 seconds. The entire pancreatic biliary tree was included in all images. The same pulse sequence was repeated to acquire 4 to 6 projections of the pancreatic biliary system from different angles.

### **3.2.2 Measurement:**

MRCP scans were obtained for various clinical indications like follow-up of abdominal trauma, abdominal pain and in a case to exclude a patients with any biliary system abnormality. The patient's age were recorded. The medical records of all patients were reviewed. Patients whose biliary system appeared abnormal on MRCP scans were excluded. Additionally, any patients who had clinical, biochemical or imaging evidence of conditions that could affect the size of the CBD and PD was excluded from the study.

### **3.2.3 Interpretation:**

By radiologist.

### **3.2.4 Data Collection and analysis:**

Data was collected using a sheet for all patients in order to maintain consistency of the information from display. A data collection sheet was designed to obtain patient gender, age, common bile duct and pancreatic duct measurement.

All measurement was registered down and from the display monitor in 1.5 TMRI scanner and then used as input to statistical software Microsoft excel for analysis and SPSS.

## **Chapter Four**

### **Results**

## Chapter Four

### Results

#### 4.1 Results:

**Table (4.1): demonstrate the distribution of the gender.**

Gender	Frequency	Percentage
Male	16	29.1
Female	39	70.9
<b>Total</b>	<b>55</b>	<b>100.0</b>

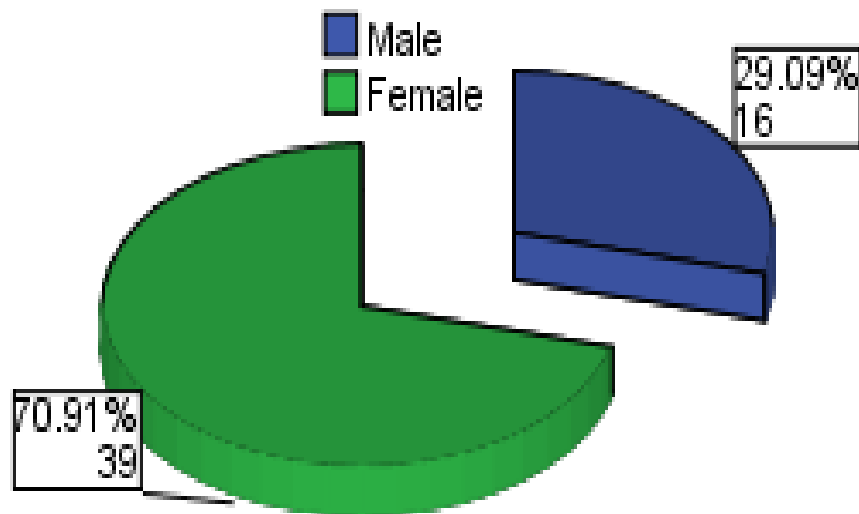


**Figure (4.1): show distribution of gender.**

**Table (4.2): demonstrate measurement of (male and female) in both Common Bile Duct and Pancreatic Duct according to Gender:**

	Gender	Mean	Std. Deviation	Std. Error Mean
Common Bile Duct (CBD)	Male	5.80	2.04	0.56
	Female	6.98	4.71	0.68
Pancreatic Duct (PD)	Male	2.35	0.43	0.12
	Female	2.58	0.83	0.12

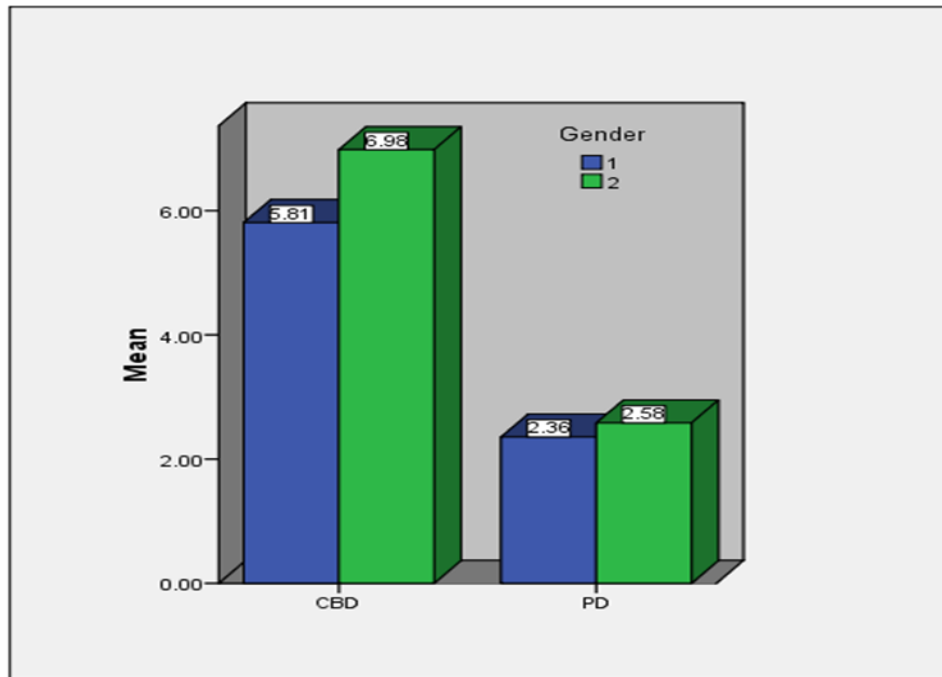


**Figure (4.2): show mean of (male and female) in both Common Bile Duct and pancreatic duct. (1 male, 2female)**

**Table (4.3): demonstrate the Measure of effect of age to (CBD) and (PD) and coefficients test.**

		Coefficients					
		B	Std. Error	t	Sig.	R	R Square
Common Bile Duct (CBD)	(Constant)	5.63	2.17	2.59	0.012	0.068	0.005
	Age	0.02	0.04	0.52	0.604		
Pancreatic Duct (PD)	(Constant)	2.19	0.38	5.64	0.000	0.115	0.013
	Age	0.007	0.008	0.89	0.376		

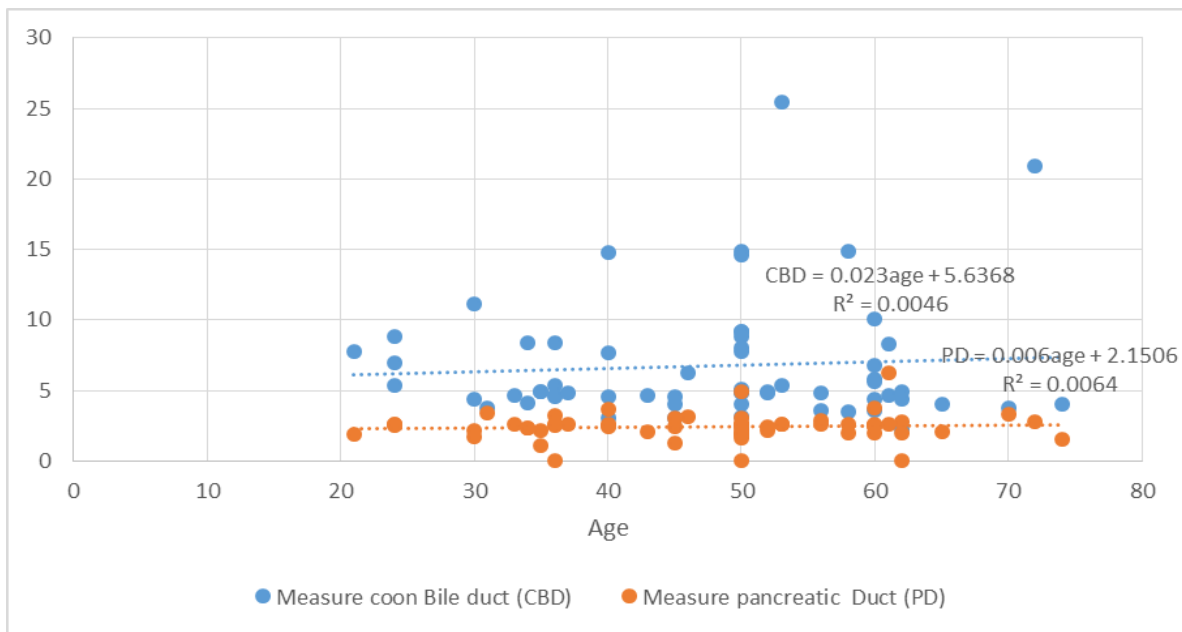


**Figure (4.3): Plots the regression of (CBD) and (PD) on age.**



**Table (4.4): demonstrate measurement of common bile duct and pancreatic duct according to age.**

	<b>Minimum</b>	<b>Maximum</b>	<b>Mean</b>	<b>Std. Deviation</b>
Age	21	74	47.66	12.66
Common Bile Duct (CBD)	2.21	25.46	6.7334	4.29
Pancreatic Duct (PD)	1.10	6.26	2.5349	.77

**Table (4.5): demonstrate the Independent samples test for equality of means of males and females in both (CBD) and (PD):**

	t-test for Equality of Means				
	t	df	Sig. (2-tailed)	Mean Difference	Std. Error Difference
Common Bile Duct (CBD)	-0.87	59	0.38	-1.17	1.34
Pancreatic Duct (PD)	-0.93	59	0.35	-0.22	0.24

## **Chapter five**

### **Discussions, conclusions and recommendations**

## Chapter five

### Discussions, conclusions and recommendations

#### 5.1 Discussions:

In this study, the age and gender related random sample of (55) patients including 16 male (29.1%) and 39 female (70.9%) from age group (21 – 78) years and that mean the females effect than male agree with Sakorafas et al( 2007). Table (4.1) and figure (4.1).

In this study, The Mean age was  $47.6 \pm 21.6$  and the mean diameter of common bile duct was ( $5.8 \pm 2.0$ mm) of male, ( $6.9 \pm 4.7$ mm) of female respectively, and the Mean diameter in pancreatic duct ( $2.3 \pm 0.4$ ) mm for male and ( $2.5 \pm 0.8$ ) mm respectively that result similar found in Tarig et al (2016). Table (4.2) and figure (4.2).

In this study the correlation( $R=0.068$ and  $0.11$ ) which indicated a very weak degree of correlation between Age and respectively the common bile duct and pancreatic duct was only 0.5% of common bile duct are due to age and only 1.3% of variation of pancreatic are due to age, (Sig'= $0.604$ and  $0.37$ ) indicate that statistically no significant correlation between age and common bile duct and pancreatic duct, (Dig Surg et al 2017).Table (4.3) figure (4.3).

In this study the average difference (Mean difference= $1.17 \pm 1.3$ mm) between the male and female for common bile duct, for the t-test statistic,  $t = -0.87$ , and Sig. (2-Tailed) = 0.38; since  $p > 0.05$  (Sig. (2-Tailed) = 0.38) ,the average difference(Mean difference =  $0.22 \pm 0.24$ ) between the male and female in Pancreatic Duct, for the t-test statistic,  $t = -0.93$ , and Sig. (2-Tailed) = 0.35; since  $p > 0.05$  (Sig. (2-Tailed) 0.35) ,there was no statistically difference between diameter of common bile duct and sex subjects.( NidhiLal et al 2014) in Table (4.5)

## **5.2 Conclusions:**

The study conclude that no different male for CBD measure, no different female CBD measure, the male and female have the same PD measure, And no correlation between diameter of CBD&PD with the age.

The results showed the mean of diameter CBD in obstructive jaundice patients are  $(6.35\pm3.35)$  mm and the mean of diameter PD for are  $(2.4\pm0.6)$  mm.

### **5.3 Recommendations:**

The study recommended that:

- Measurement in different area in CBD at (begin, middle, end).
- Radiologist and physician use the sander size in diagnosis the common bile duct and pancreatic duct abnormalities.
- Further studies in measuring common bile duct and pancreatic duct with larger sample of population.
- Further imaging modalities like U/S and ERCP should be used for measuring the common bile duct and pancreatic duct.

## References

Alexandre, L et al the ABC of MRCP Bachar,G. n. et al (2003): effect of aging on the adult extrahepatic bile duct a Sonographic study. The American institute of ultrasound in medicine. 22 p 879–882.

Barbara, I. et al (1987) a population study on the prevalence of gallstone disease: the sirmione study. Hepatology. Sep-oct; 7.(5):p7-13.

Bernstein, M.A. et al (2004): hand book of MRI pulse sequence 1<sup>st</sup>ed. elsevier inc.

Chen, T. et al. (2012) the diameter of the common bile duct in an asymptomatic taiwanese population: measurement by magnetic resonance cholangiopancreatography journal of the chinese medical association 75. P 384-388.

Dahlstrom, n. (2009): magnetic resonance imaging of the hepatobiliary system using hepatocyte-specific contrast media. 1<sup>st</sup>ed linköping, sweden, 2009.

Fargulidis, et al. (2008) managing injuries of hepatic duct confluence variants after major hepatobiliary surgery: an algorithmic approach. world j gastroenterol may 21; 14(19):p 3049-3053

Federal, M P (2004) diagnosing imaging abdomen. 1<sup>st</sup>ed salt lake city.

Amirsysinc Fulcher, A.S. (1999). MR cholangiography technical advances and clinical application. radiographics 12 (1) p 25-44.

Gulati, k et al. (2007). Review: advances in magnetic resonance cholangiopancreatography: from morphology to functional imaging. Indian j. radiol imaging. 17 (4) p 247-253.

Håkansson, k. et al. (2002). On the appearance of bile in clinical MR cholangiography. ACTA radiologica 43 401–410.

Harrow, M.M. (2010) ultrasound of the extrahepatic bile duct issues of size. *Ultrasound quarterly*. 26, (2). P 67-74.

Hung, C.R. et al (2011) common bile duct diameter measurement by magnetic resonance cholangiopancreatography. *J radiol sci June vol.36 no.2* p 93-97.

Hyodo, T et al (2012): review article CT and MR cholangiography: advantages and pitfalls in preoperative evaluation of biliary tree. *The British journal of radiology*, 85(2012), 887–896.

Jensen, P.F. et al (2006): evaluation of the biliary tract in patients with functional biliary symptoms. *World j gastroenterol* 14; 12(18): p 2839-2845.

John, M.A. et al emergency ultrasound 2nd ed. mcgraw-hill access surgery.

Kantarci, M. et al (2013) non-invasive detection of biliary leaks using gadolinium-enhanced MR Cholangiography: comparison with T2-weighted MR cholangiography. *eur radiol* 23.p 2713–2722.

Khuroo, M.S. et al: (1989) liver, biliary and pancreas prevalence of biliary tract disease in India: a sonographic study in adult population in Kashmir. Published by group.bmj.com.

Kumar et al. (2004) Robbins and Cotran the pathologic basis of disease. 7th ed. Elsevier.

Lee, H.C. et al: (2000) dilatation of the biliary tree in children: sonographic diagnosis and its clinical significance. *American institute of ultrasound in medicine j ultrasound med* 19:p 177–182.

Maccioni, F. et al (2010) magnetic resonance cholangiography: past, present and future. *European review for medical and pharmacological sciences*. 14: p 721-725.

Majeed, A. W. (1999). The preoperatively normal bile duct does not dilate after cholecystectomy: results of a five year study downloaded from gut.bmj.com. 45:741–743.

Mandarano. G et al. (2008) the diagnostic MRCP examination: overcoming technical challenges to ensure clinical success. *Biomedical imaging and intervention journal* 4(2):e 28.

Matthew,A.B.et al: (1999) magnetic resonance cholangiopancreatography. *The New England journal of medicine* July 22. P -258-264.

Mortar,K.J. and Ross,P.R. (2001) anatomic variants of the biliary tree: MR cholangiographic findings and clinical applications. *American roentgen ray society*: 177: p 389–394.

Nuray. et al. (2009). Normal biliary confluence angle in classical junction type: assessment with MR Cholangiopancreatography: *ankara universitesi tip fakultesi mecmuasi*,62(4).

Palmer,P.E.S (2005): manual of diagnostic ultrasound.geneva. world health organization

Park,S. M. et al (2012) common bile duct dilatation after cholecystectomy: a one-year prospective study. *Journal of the Korean surgical society*: 83p 97-101.

Pierre,E.C and Laillie, j. (2013): diseases of the gallbladder and bile ducts: diagnosis and treatment. 1<sup>st</sup> ed john wiley & sons.

Roport,S.P et al. (2000): common bile duct measurements in an elderly population *j ultrasound med* 19:727–730.

Sales. D.M. et al (2009) evaluation of morphological changes of the biliary tree by magnetic resonance cholangiography in patients with schistosomiasis mansoni: interobserver agreement. *Radiol bras.set/out*; 42(5): p 277–282.

Sanyal.R. et al (2012) secretin-enhanced MRCP: review of technique and application with proposal for quantification of exocrine function. *ajr* january: 198, p 124-132.

Skandalaki J. E. et al (2008): skandalakis' surgical anatomy. 4<sup>th</sup> ed mcgraw-hills access surgery.



Soto, y. A. et al (1995):MRcholangiopancreatography: findings on3d fast spin-echo imaging AJR; American roentgen ray society165:1397

Standring,S (2008): gray anatomy the anatomical basis ofclinical practice. 39th ed. elsevierchurchillLivingston

Tes,F. et al (2006): non-operative imaging techniques insuspected biliary tract obstruction. Taylor&Francis. 8: 409-425.

Thomson,A.B.R. and Shaffer,E.E (2005): first principleof gastroenterology the basis of the disease and anapproach to management. 1st ed.

janssenortho.Westbrook,C. et al. (2005) MRI practice. 3rd ed. oxford:blackwell publishing.

Diagnostic imaging by peter Armstrong Martin L.wastie ,fourth edition 1998.

Tarig Mawyaia Haga Abukhir (2016) M.sc degree of Sudan University of sciences and technology faculty of radiology.

Regan j.Breg,MD et al(2017) university of southern California ,KAC+USC medical center

# Appendix



**Cases of research:**

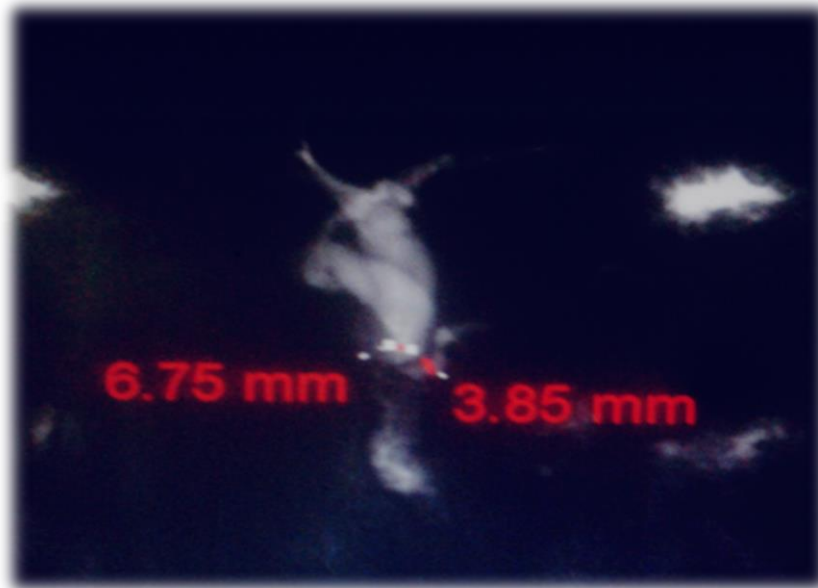


**Image (1): 49 years female demonstrate CBD with obstructive jaundice and pancreatic duct measurement on MRCP image.**



**Image (2): 40 years male demonstrate CBD and pancreatic duct measurement on MRCP image.**